

# Use Of Geophysical Profiling To Guide Groundwater Remediation Studies

David B. Watson, William E. Doll, T. Jeffrey Gamey, and Philip M. Jardine,  
*Environmental Sciences Division*  
*Oak Ridge National Laboratory*  
*PO Box 2008*  
*MS 6038*  
*Oak Ridge, TN 37831-6038*  
[watsondb@ornl.gov](mailto:watsondb@ornl.gov)

**Abstract**—*Multielectrode resistivity methods and pseudo-tomographic seismic refraction techniques were used to image to a depth of approximately 30 m at the Natural and Accelerated Bioremediation Research Field Research Center, a research site that has been developed by the U. S. Department of Energy to study bioremediation methods. The site is known to contain nitrates, uranium, and other contaminants. These geophysical methods were effective in delineating the plume and in defining geologic units that appear to influence contaminant transport. Extensive drilling and groundwater sampling verified the geophysical data.*

## I. INTRODUCTION

The U. S. Department of Energy (DOE) has initiated research at the Field Research Center (FRC) on the Oak Ridge Reservation (ORR), Tennessee as part of the Natural and Accelerated Bioremediation Research (NABIR) program to develop and evaluate bioremediation tools for contaminated sites. The FRC includes a contaminated field site and an uncontaminated Background Area, both located in Bear Creek Valley (BCV) west of the Oak Ridge Y-12 National Security Complex. The FRC contaminated field site has been divided into 3 areas available for NABIR researchers to

conduct bioremediation field studies. Liquid wastes, composed primarily of nitric acid plating wastes containing nitrate and various metals and radionuclides (e.g., uranium and technetium) were disposed of in the S-3 ponds until 1983. Waste disposal activities at the site have created a large mixed waste plume of contamination in the underlying unconsolidated saprolite and more competent shale bedrock. The ponds were neutralized and denitrified in 1984, and capped under the Resource and Conservation Recovery Act (RCRA) to reduce infiltration of rainfall and flow of contaminants into the groundwater system.

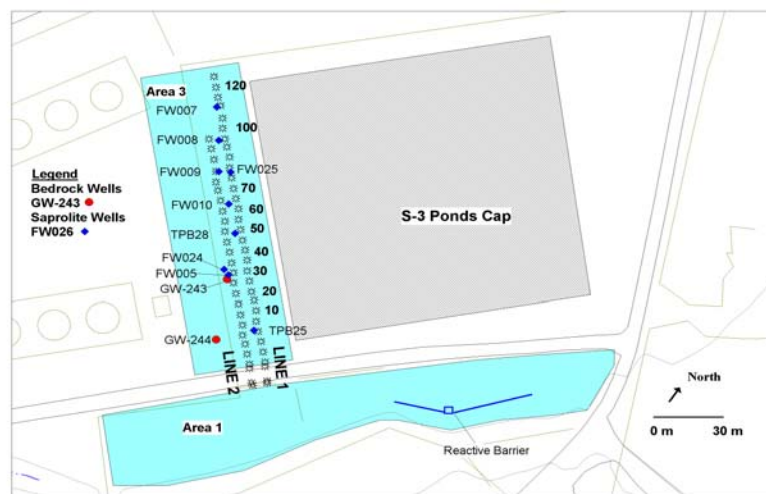
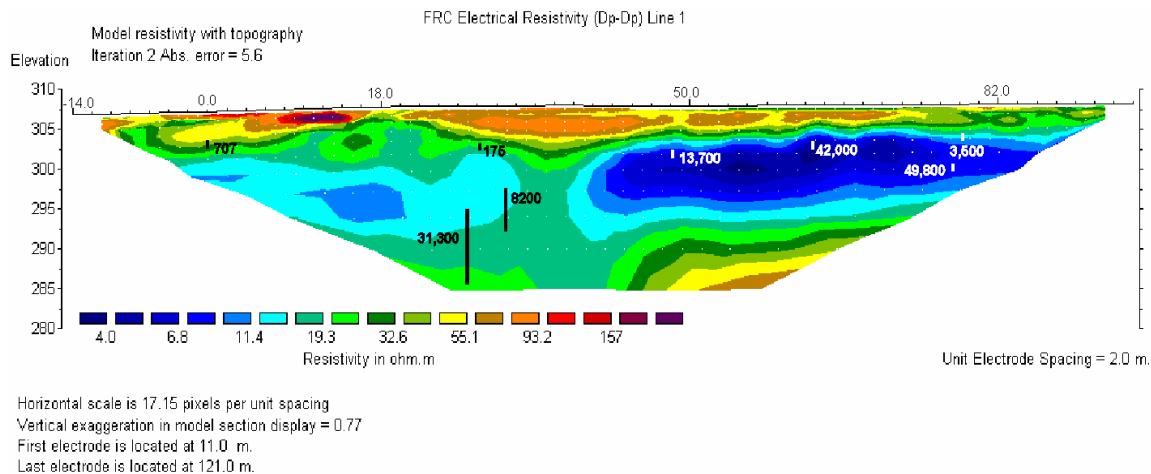


Figure 1. Site map, showing Area 3, adjacent features, and geophysical survey lines.



**Figure 2.** Multielectrode resistivity section (dipole-dipole) for Line 1. Measured nitrate concentrations (in mg/l) are superimposed on the section along with lines that depict the screen interval from which the nitrate samples were acquired.

Selection of appropriate field scale research plots for the FRC requires as much information as possible about the location of the plume and the geologic structures that control its distribution in three-dimensional space. Typically this information has been derived by drilling a series of expensive monitoring wells and analyzing samples at regular depth intervals within the wells. In this case, geophysical measurements were used to reduce the extent of drilling, reduce costs, and assure continuity between wells. Geophysical data were acquired in Area 3 (Figure 1) located immediately adjacent to the west side of the former S-3 Disposal Ponds (Doll et al., 2002)<sup>1</sup>.

## II. TECHNICAL DESCRIPTION

To detect the high ionic strength plume and geologic structures, we conducted a multielectrode resistivity survey with a Sting/Swift 56-electrode system with 1 m and 2 m electrode separations in both dipole-dipole and Schlumberger configurations. Processing of the resistivity data was done with AGI-2Dinv software.

Several tomographic or pseudo-tomographic seismic refraction software products are currently available for imaging geologic structures in two dimensions. Seismic methods are largely insensitive to the presence or absence of contaminants except where their fluid properties may have subtle effects on velocity and reflectivity. They can however have greater depth penetration than the multielectrode resistivity methods. These seismic methods use dense shot patterns and large geophone arrays to provide a data set that can be inverted for velocity over a grid of points in a profile. The constant velocity and/or continuous layer restrictions of conventional delay-time or generalized reciprocal methods can thus be relaxed to yield a profile that is more representative of many near-surface environments.

Seismic data were acquired with a weight drop source and 1m geophone spacing and were processed using Rayfract software.

## III. RESULTS

Seismic and resistivity data were both acquired on Line 1 and Line 2 (Figure 1). The resistivity section for Line 1 is shown in Figure 2, annotated with nitrate concentrations measured in several monitoring wells. Figure 3 shows the seismic velocity contours superimposed on the equivalent portion of the resistivity section from Figure 2. In general, the seismic section provides indication of structural changes in the soil and weathered bedrock. The resistivity is sensitive to these effects, but even more sensitive to the ionized fluids in the plume. Where both methods show anomalous behavior, it is presumably because the anomalous measurements are due to a structural feature, or the plume location is controlled by a structural feature. Steep gradients or changes in gradient in seismic velocity are often indicative of interfaces between two structural regimes.

The primary region of interest for the FRC is the top 15-20 m of the section. Selected seismic velocity contours can be used to differentiate zones in the section. A steep velocity gradient occurs between  $x=20$  m and  $x=30$  m in the top 2-3 m of the section where velocities increase from 500 m/s to 1000 m/s and reach 1000 m/s shallower than in the adjoining portions of the section. Velocities are higher beneath this zone to a depth of about 6 m (301 m elevation). We associate the lateral variability in the top 3-6 m as being due to differences between fill materials vs. naturally weathered rock. A lens-shaped zone of lower vertical velocity gradient and lateral velocity discontinuity occurs roughly between the 1500

m/s contour and the 2000 m/s contour. Within this region, lateral velocity changes of a few hundred m/s are common over distances of a few meters, presumably indicating heterogeneity. Between the 2000 m/s contour and the 3000 m/s or 3500 m/s contours, there is a transition to a zone of steep gradients with lateral

discontinuities. This zone may represent the transitional weathered fractured bedrock between the highly weathered saprolite and bedrock that is largely unweathered.

There are several similarities between the seismic and resistivity results. The low velocity portions of the seismic section in the top 3-5 m correspond in location and general shape with resistivities greater than 50 ohm-m in the resistivity section. The conducting region between 292 and 301 m in the resistivity section shows strong correlation with the region of lateral heterogeneity bounded by the 1500 m/s and 2000 m/s contours in the seismic section. At depth, increases in resistivity are generally associated with increases in velocity or strong gradients in the seismic velocity. This may be an indication of unweathered bedrock.

We used the integrated seismic and resistivity data to formulate hypotheses regarding the probable areas of contaminant transport. Our intent was to locate and establish a field facility for investigating the subsurface processes that control the microbially mediated reduction and subsequent immobilization of uranium. The resolution of the geophysical measurements was sufficient for guiding the spatial location and depth of numerous

groundwater sampling wells. Seismic refraction tomography was used to estimate the vertical extent of auger penetration and electrical resistivity was used to target subsurface regimes where elevated concentrations of uranium and  $\text{NO}_3^-$  were suspected. Three groundwater monitoring wells, namely FW010, FW024, and FW005, were situated in regimes indicative of high, moderate, and low resistivity, respectively (Figure 1 and Table I). Groundwater nitrate concentrations from the three wells agreed extremely well with the electrical resistivity measurements where high, moderate, and low resistivity regimes contained 44248, 8200, and 175 mg/L  $\text{NO}_3^-$ , respectively.

Groundwater geochemistry in the vicinity of FW024 was scientifically appealing and multilevel wells were installed for flow and chemistry monitoring. A bladder pump was situated in a straddle packer design for measuring groundwater flux via a point-dilution technique, and geochemistry as a function of depth. The results suggested that 90-95% of groundwater flow was within the 9.1 to 13.7 m depth interval (298 to 293 m elevation) and that groundwater U and  $\text{NO}_3^-$  concentrations were nearly uniform from 6.1 to 13.7 m. (303 to 292 m elevation). These data agreed extremely well with the geophysical measurements (Figures 2 and 3). The lens of low vertical seismic velocity gradient and laterally varying velocities at 293 m to 298 m elevation appears to be associated with a poorly consolidated zone of enhanced groundwater flow. This was consistent with groundwater flux measurements, which suggested that the bulk of groundwater flow occurred within this regime.

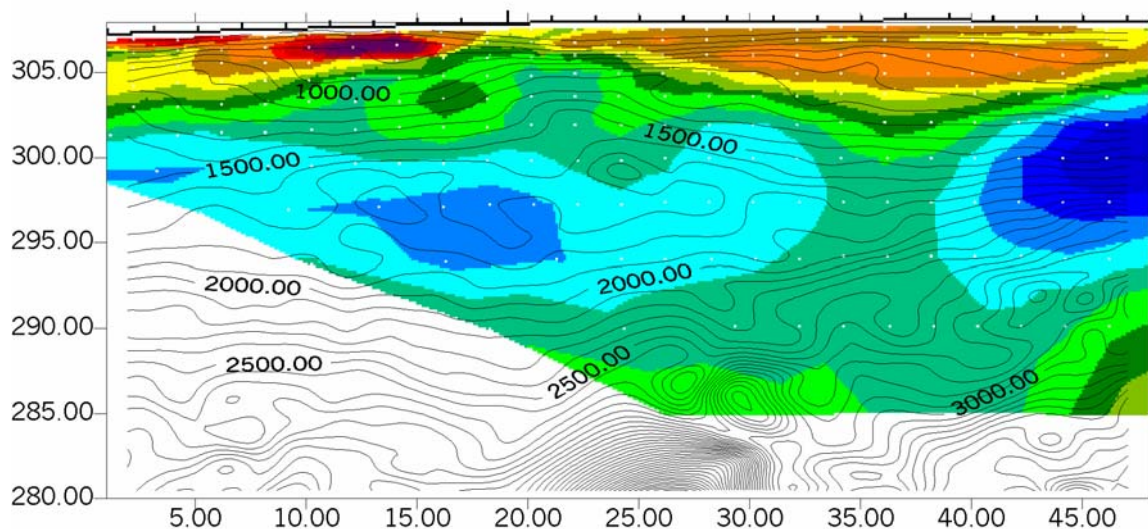


**Figure 3.** Integrated seismic and resistivity map for a portion of Line 1. Seismic velocity contours (in m/s) are overlain on the equivalent portion of the resistivity cross-section of Figure 2. Color-coding for the resistivity contours are the same as in Figure 2.

Well ID	Distance on Resistivity Section (m)	Depth Range (m)	Measured Nitrate Concentration (mg/l)	Measured Fluid Resistivity ( $\Omega$ m)	Resistivity from Sting Survey ( $\Omega$ m)
GW-244	-1	13.1-22.9	-	0.36	-
TPB25	0	4.6	707	1.4	26-30
GW-243	27	13.1-22.3	31,300	0.32	14-22
FW005	28	5.2	175	6.2	14-22
FW024	31	15.2	8,200	0.23	16.5
TPB28	48	6.1	13,700	0.70	6
FW010	63	6.7	44,248	0.20	3.9
FW025	77	7.6	49,800	0.24	7.5
FW009	78	4.6	3,461	1.5	9.9
FW008	94	3.4	110	1.3	11
FW007	110	3.0	6,987	0.78	-

Table I. Comparison of Fluid Resistivity with Sting Survey Resistivities

The base of this zone, which correlates roughly with the 2000 m/s velocity contour underlain by higher vertical velocity gradients, is associated with auger refusal at the weathered bedrock interface (Figure 3). Groundwater uranium and  $\text{NO}_3^-$  concentrations were homogeneous from an elevation of 303 to 293 m in well FW024, with a sharp drop in concentration occurring above 303 m. Again, these results were consistent with the electrical resistivity data that showed uniform low resistivity between 302.5 and 293 m, and increasing resistivity above 302.5 m (Figures 2 and 3).

#### IV. DISCUSSION AND ANALYSIS

##### *IV.i. Seismic Representation of the Water Table*

We note that the zones that we interpret as containing ionized groundwater extend above the 1500 m/s velocity contour, a velocity that is typically associated with the water table. Several explanations for this apparent inconsistency can be provided; all are associated with the acquisition and analysis of the seismic data, or features of the algorithms that were used in processing. These include 1) possible delayed picks of first breaks; 2) a tendency of the Delta t-V method to smear abrupt gradients; 3) movement of the water table between acquisition of seismic data and acquisition of resistivity data; 4) poor constraint of the surface layer due to air wave interference or too few channels, and 5) insufficient data coverage at the north end of the profile line. More importantly, the water table often correlates with a velocity that is lower than the 1500 m/s rule-of-thumb. According to Hasselstroem (1969)<sup>2</sup>, the transition occurs in the velocity range of 1200-1800 m/s in porous materials. Haeni (1986)<sup>3</sup> notes a similar transition for New England glacial materials. A tomographic study of a groundwater contamination site near Ogden Utah shows

the water table corresponding to a velocity of 1100-1200 m/s (Zelt et al., 2002)<sup>4</sup>.

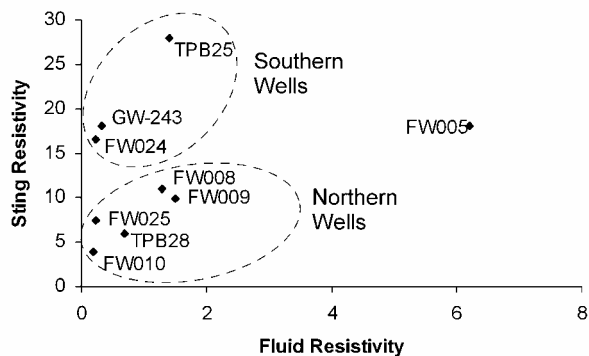
##### *IV.ii. Relationship between Nitrate Concentrations and Resistivity*

Table I shows the nitrate concentrations that were overlain on Figure 2 along with measured fluid resistivities and resistivities derived from the inverted multielectrode resistivity survey. The measured fluid resistivities are commonly related to the effective resistivities, as measured by a multielectrode resistivity survey, by Archie's Law (Reynolds, 1997)<sup>5</sup>,

$$\rho = a \phi^{-m} s^{-n} \rho_w,$$

where  $\rho$  is the effective resistivity,  $\rho_w$  is the pore fluid resistivity,  $s$  is the volume fraction of fluid-filled pores,  $\phi$  is the porosity, and  $a$ ,  $m$ , and  $n$  are constants. In effect, the matrix resistivity is considered negligible. Archie's Law may not be reliable where clay minerals are abundant (Parasnis, 1986)<sup>6</sup>, as in the saprolite layer. The value of  $n$  is about 2 where more than 30% of pore space is fluid filled. Typical values for the other two constants are  $0.5 < a < 2.5$  and  $1.3 < m < 2.5$ .

Figure 4 shows the fluid resistivity values in Table I plotted against the corresponding resistivities derived from the relevant portion of the inverted Sting data. Taken as a whole, there is a great deal of scatter in the points. However, if the data from the three southernmost wells (TPB25, GW-243, and FW024) are separated from those from the northern wells, the two groups would fit lines with much higher correlation coefficients. The southern well measurements are all from an apparent southern lobe of the plume that may be distinct from the northern lobe, as indicated by the discontinuity in the low resistivity (blue) layer at about  $x=35$  m. FW005 is not clearly associated with either group, though it appears that it could fall close to the projection of a line that could be fit to northern wells. It represents a sample from the shallow depth regime that could be distinct from either of the other two groups.



**Figure 4.** Plot of fluid resistivities vs. Sting resistivities from Table I. The points can be divided into two groups, providing evidence for a fundamental change in saprolite properties between the southern area and the northern area of the profile.

We interpret Figure 4 to indicate that there are at least two distinct material types at the site which differ in chemistry, porosity, pore volume, or in other properties that affect the values of the constants,  $a$ ,  $m$ , and  $n$ . The distinction may have to do with differences in the ratio of other ions to nitrates, in clay content, between in situ and fill materials, or in the mineralogy or weathering properties of the lithologies that outcrop at the site. Differences in the amounts of other ionic contaminants are known to exist between these two areas. Observations made during the drilling of these wells indicates that the material in the south tends to be more highly leached and weathered from the migration of the acidic wastes from the S-3 Ponds. This extends to a greater depth than in the north. The northern wells are adjacent to a different pond (four ponds were covered by the cap) than the southern wells and each pond may have contained wastes of a different composition. We are assessing the impact that this might have on the geophysical data. Weathered Nolichucky shale exhibits variations in silt and clay content (Hatcher et al., 1992)<sup>7</sup> that could affect its porosity or other properties along these survey lines, which are oriented perpendicular to strike. Because the beds dip at about  $45^\circ$ , material changes could occur over a short distance. The change in material properties might also be inferred from the seismic velocities. High velocities appear to shallow toward the north end of the seismic line (Figure 3). This agrees with a shallower depth of refusal for push-probe wells in this area, where harder saprolite/bedrock was encountered at a shallower depth. Additional seismic work is planned to characterize the northern portion of Line 1.

## V. CONCLUSIONS

The integrated seismic and resistivity geophysical techniques provided a rapid and effective method for defining the spatial location of contaminant plumes. These techniques not only save time and money by guiding the installation of groundwater sampling wells, they also provide enhanced subsurface spatial resolution over well data such that the likelihood of missing a significant contaminant plume is reduced.

## ACKNOWLEDGEMENTS

We gratefully acknowledge Siegfried Rowdewald, Intelligent Resources Inc., for providing guidance in using the Rayfract software, and in assessing the result. Jon Nyquist (Temple University) provided guidance in using the Sting/Swift system. Barry Kinsall and Ken Lowe provided field assistance. This research was supported by the US Department of Energy's Office of Science and is a contribution from the Natural and Accelerated Bioremediation Research (NABIR) program, of the Office of Biological and Environmental Research (BER). Oak Ridge National Laboratory is managed by UT-Battelle, LLC for the U. S. Department of Energy under contract DE-AC05-00OR22725. The submitted manuscript has been authored by a contractor of the U. S. Government. Accordingly, the U. S. Government retains a nonexclusive, royalty-free license to publish or reproduce the published form of this contribution, or allow others to do so, for U. S. Government purposes.

## REFERENCES

1. DOLL, W.E., T.J. GAMEY, D.B. WATSON, AND P.M. JARDINE. 2002. *Geophysical Profiling In Support Of A Nitrate And Uranium Groundwater Remediation Study, Extended Abstracts. 2002 Symposium on the Application of Geophysics to Engineering and Environmental Problems, Las Vegas, NV. Feb. 10-14, 2002*, 10p.
2. HASSELSTROEM, B. 1969. "Water Prospecting and Rock-investigation By the Seismic Refraction Method." *Geoexploration*. 7:113 (1969).
3. HAENI, F.P. 1986. "Application of Seismic Refraction Methods in Groundwater Modeling Studies in New England." *Geophysics*. 51:236 (1986).

4. ZELT, C., A. LEVANDER, A. AZARIA, D. DANA, AND I. MOROZOV. 2002. "3-D Seismic Tomography at a Groundwater Contamination Site" <http://terra.rice.edu/department/research/colin2/colin2.html>.
5. REYNOLDS, JOHN M. 1997. *An Introduction to Applied and Environmental Geophysics*. (J. Wiley and Sons, 796 p., 1997).
6. PARASNIS, D.S., 1986, *Principles of Applied Geophysics*. (Methuen and Co., Ltd., New York, 402 p., 1986).
7. HATCHER, R.D. JR., P.J. LEMISZKI, R.B. DREIER, R.H. KETELLE, R.R. LEE, D.A. LEITZKE, W.M. MCMASTER, J.L. FOREMAN, AND S.Y. LEE. 1992. "Status Report on the Geology of the Oak Ridge Reservation." ORNL/TM-12074, Martin Marietta Energy Systems, October 1992, 244 p.